



HAL
open science

Independent Regulation of Symbiotic Nodulation by the SUNN Negative and CRA2 Positive Systemic Pathways

Carole Laffont, Emeline Huault, Pierre Gautrat, Gabriella Endre, Peter Kalo, Virginie Bourion, Gérard Duc, Florian Frugier

► **To cite this version:**

Carole Laffont, Emeline Huault, Pierre Gautrat, Gabriella Endre, Peter Kalo, et al.. Independent Regulation of Symbiotic Nodulation by the SUNN Negative and CRA2 Positive Systemic Pathways. *Plant Physiology*, 2019, 180 (1), pp.559-570. 10.1104/pp.18.01588 . hal-02404353

HAL Id: hal-02404353

<https://hal.science/hal-02404353>

Submitted on 17 Dec 2020

HAL is a multi-disciplinary open access archive for the deposit and dissemination of scientific research documents, whether they are published or not. The documents may come from teaching and research institutions in France or abroad, or from public or private research centers.

L'archive ouverte pluridisciplinaire **HAL**, est destinée au dépôt et à la diffusion de documents scientifiques de niveau recherche, publiés ou non, émanant des établissements d'enseignement et de recherche français ou étrangers, des laboratoires publics ou privés.

Independent Regulation of Symbiotic Nodulation by the SUNN Negative and CRA2 Positive Systemic Pathways¹

Carole Laffont,^a Emeline Huault,^a Pierre Gautrat,^a Gabriella Endre,^b Peter Kalo,^c Virginie Bourion,^d Gérard Duc,^d and Florian Frugier^{a,2,3}

^aInstitute of Plant Sciences Paris-Saclay, Centre National de la Recherche Scientifique, Université Paris Sud, Université Paris Diderot, Institut National de la Recherche Agronomique, Université d'Evry, Université Paris-Saclay, 91190 Gif-sur-Yvette, France

^bInstitute of Plant Biology, Biological Research Centre, 6726 Szeged, Hungary

^cNational Agricultural and Innovation Center, Agricultural Biotechnology Institute, 2100 Godollo, Hungary

^dAgroécologie, Institut National de la Recherche Agronomique, AgroSup Dijon, Université Bourgogne Franche-Comté, 21065 Dijon, France

ORCID IDs: 0000-0002-8447-1736 (C.L.); 0000-0002-0404-8904 (P.K.); 0000-0002-2921-3152 (G.D.); 0000-0002-9783-7418 (F.F.).

Plant systemic signaling pathways allow the integration and coordination of shoot and root organ metabolism and development at the whole-plant level depending on nutrient availability. In legumes, two systemic pathways have been reported in the *Medicago truncatula* model to regulate root nitrogen-fixing symbiotic nodulation. Both pathways involve leucine-rich repeat receptor-like kinases acting in shoots and proposed to perceive signaling peptides produced in roots depending on soil nutrient availability. In this study, we characterized in the *M. truncatula* Jemalong A17 genotype a mutant allelic series affecting the Compact Root Architecture2 (CRA2) receptor. These analyses revealed that this pathway acts systemically from shoots to positively regulate nodulation and is required for the activity of carboxyl-terminally encoded peptides (CEPs). In addition, we generated a double mutant to test genetic interactions of the CRA2 systemic pathway with the CLAVATA3/EMBRYO SURROUNDING REGION peptide (CLE)/Super Numeric Nodule (SUNN) receptor systemic pathway negatively regulating nodule number from shoots, which revealed an intermediate nodule number phenotype close to the wild type. Finally, we showed that the nitrate inhibition of nodule numbers was observed in *cra2* mutants but not in *sunm* and *cra2 sunm* mutants. Overall, these results suggest that CEP/CRA2 and CLE/SUNN systemic pathways act independently from shoots to regulate nodule numbers.

Plant growth capacity is linked to the developmental plasticity of the root system, allowing acclimatization to heterogenous and changing soil nutrient availability and stress environmental conditions (Malamy, 2005; Giehl and von Wirén, 2014). These extrinsic signals are perceived locally and relayed by endogenous cues that can act either locally and/or at long distance through the whole plant (De Kroon et al., 2009). This implies that

systemic signaling pathways acting between organs through the vasculature allow an integration of local environmental conditions and the coordination of root and shoot metabolism, development, and growth. These systemic pathways are critical to allow plants to optimize nutrient uptake and to set up a foraging behavior adapted to local environmental conditions (De Kroon et al., 2009; Giehl and von Wirén, 2014). Root system architecture is determined by root growth and branching to generate lateral roots. Various endogenous cues have been shown to locally and systemically regulate root system architecture, including nonpeptide and peptide hormones (Malamy, 2005; Giehl and von Wirén, 2014). Among those, CLAVATA3/EMBRYO SURROUNDING REGION (CLE)-secreted signaling peptides are produced within a specific domain of *Arabidopsis* (*Arabidopsis thaliana*) shoot and root apical meristems and act locally on stem cell division and/or differentiation (Tavormina et al., 2015; Oh et al., 2018). These CLE peptides bind to the CLAVATA1 leucine-rich repeat receptor-like kinase (LRR-RLK) that is specifically expressed in a neighboring domain as the one where CLE peptides are produced, allowing the definition of positional information. A related CLE/LRR-RLK signaling module involving CLE peptides induced

¹This work was supported by the French-Hungarian bilateral NKTH-ANR LEGUMICS project (TÉT_10-1-2011-0397) and the ANR (2010-INTI3-1602-01 project) as well as the Hungarian National Research Fund (OTKA-105852). P.G. was supported by a fellowship from the Paris Sud/Paris-Saclay University and E.H. by the LEGUMICS ANR project.

²Author for contact: florian.frugier@cnrs.fr.

³Senior author.

The author responsible for distribution of materials integral to the findings presented in this article in accordance with the policy described in the Instructions for Authors (www.plantphysiol.org) is: Florian Frugier (florian.frugier@cnrs.fr).

F.F. designed the study; C.L., E.H., and P.G. performed the experiments; G.E., P.K., V.B., and G.D. provided the genetic material; C.L. and F.F. wrote the article.

www.plantphysiol.org/cgi/doi/10.1104/pp.18.01588

by N deficiency was more recently shown to repress lateral root primordia expansion, therefore contributing to the regulation of root foraging responses, and was proposed to act systemically (Araya et al., 2014a, 2014b).

In legume (Fabaceae) plants, the root system forms another type of lateral organ, the symbiotic N-fixing nodule (Oldroyd, 2013; Suzaki et al., 2015), which is a metabolic and developmental adaptation to N-limiting conditions. Root nodules are formed following a symbiotic interaction with specific soil bacteria collectively referred to as rhizobia. Nodule initiation relies on the coordination of different processes: first, the perception of environmental conditions permissive for symbiotic nodulation, namely, a limited soil N availability and the presence of compatible rhizobia; second, rhizobial infections initiating in epidermal root hairs and leading to the formation of infection threads (ITs) that allow bacteria to progress from root hairs to root inner cortical cell layers; and third, an organogenesis program that is simultaneously initiated, involving cortical and pericycle cell divisions as well as the breaching of the endodermis to form a nodule primordium that will be reached by ITs filled with rhizobia progressing from root outer cell layers (Timmers et al., 1999; Xiao et al., 2014). The nodule primordium then differentiates into a mature nodule in which symbiotic bacteria fix atmospheric N into ammonium, an N source that can be metabolized by plant cells. The interaction between plant and rhizobia initiates a molecular dialog where N-limited plants secrete flavonoids that attract bacteria, which in turn produce nodulation factors (NFs; Oldroyd, 2013; Suzaki et al., 2015). Perception of NFs by the plant triggers the transcriptional regulation of nodulation genes, so-called early nodulin genes, such as *EARLY NODULIN11* (*ENOD11*) that is expressed at symbiotic recognition (preinfection) and infection stages (Journet et al., 2001). *ENOD11* is therefore considered as a quantitative marker to evaluate the strengths of early symbiotic signaling and infection responses to rhizobia.

Nodule formation is an energy-consuming process that plants tightly control for costs and benefits depending on their photosynthetic capacities or on soil N availability (Suzaki et al., 2015). A regulatory pathway negatively controlling nodule number, so-called Autoregulation of Nodulation (AON; Caetano-Anollés and Gresshoff, 1991), was initially characterized through the identification of hypernodulation or supernodulation mutants that were affected in an LRR-RLK from the subclass XI acting in shoots, as shown by grafting experiments. This receptor is most closely related to the Arabidopsis CLAVATA1 protein and is referred to as Super Numeric Nodules (SUNN) in *Medicago truncatula*, Hypernodulation and Aberrant Root in *Lotus japonicus*, and Nodule Autoregulation Receptor Kinase in soybean (*Glycine max*; Krusell et al., 2002; Searle et al., 2003; Schnabel et al., 2005). The current AON model proposes that the expression of CLE

peptide-encoding genes is induced at an early nodulation stage, such as *CLE12* and *CLE13* in *M. truncatula*, *CLE-Root Signal1* (*CLE-RS1*), *CLE-RS2*, and *CLE-RS3* in *L. japonicus*, and *Rhizobia-Induced CLE1* (*GmRIC1*) and *GmRIC2* in soybean (Okamoto et al., 2009; Mortier et al., 2010; Reid et al., 2011; Nishida et al., 2016). More recently, additional *CLE* genes regulated by rhizobium inoculation were identified (Jardinaud et al., 2016; de Bang et al., 2017; Imin et al., 2018; Hastwell et al., 2019). These peptides would be then translocated from nodulated roots to shoots through the xylem vasculature to bind the LRR-RLK receptors previously mentioned (Okamoto et al., 2013; Suzaki et al., 2015; Imin et al., 2018). Integration of shoot metabolic signals would modulate the production of shoot-to-root systemic signals moving across the phloem to inhibit the formation of additional supernumerary nodules (Suzaki et al., 2015). A striking feature of the supernodulation/hypernodulation mutants is that the excessive nodulation phenotype is also observed under high-nitrate conditions that are inhibitory to the wild-type plant nodulation (Carroll et al., 1985; Sagan et al., 1995; Krusell et al., 2002; Schnabel et al., 2005; Judy et al., 2010; Okamoto and Kawaguchi, 2015). This suggested that AON and nitrate inhibitory pathways may be at least partially overlapping.

A second systemic pathway acting from shoots to positively regulate nodulation was more recently identified in the *M. truncatula* model. The *cra2* (*compact root architecture2*) mutant identified in the R108 genotype indeed forms a reduced number of nodules but also an increased number of lateral roots (Huault et al., 2014). The *CRA2* gene encodes an LRR-RLK receptor from the same subclass XI as SUNN, and grafting experiments indicated that *CRA2* positively controls nodule number from shoots and negatively controls the number of lateral roots from roots. The expression of genes encoding another family of secreted signaling peptides than CLE, referred to as CEPs (for C-terminally Encoded Peptides), was found to be mostly associated with N deficiency conditions, and exogenous applications of MtCEP1 peptides negatively regulated lateral root formation and positively regulated nodulation (Imin et al., 2013). Interestingly, these exogenous applications of MtCEP1 peptides required the *CRA2* receptor to regulate both nodule and lateral root number (Mohd-Radzman et al., 2016). Accordingly, the LRR-RLK most closely related to *CRA2* in Arabidopsis is a CEP Receptor (CEPR1) directly binding AtCEP1 peptides to regulate N-demand signaling (Tabata et al., 2014). This highlights that in *M. truncatula* also, CEP peptides are likely candidates to be *CRA2* ligands, although no direct binding evidence has been provided yet (Mohd-Radzman et al., 2016).

Altogether, these results indicate that at least in the *M. truncatula* model legume, two systemic pathways regulate the number of nodules from shoots: under N-limiting conditions, the CEP/*CRA2* pathway positively regulates nodulation, whereas during

nodule formation, activation of the CLE/SUNN negative AON pathway limits the number of additional nodules formed. Plants are continuously challenged by fluctuating environmental conditions (Giehl and von Wirén, 2014): different parts of root and shoot systems perceive spatial heterogeneity for beneficial or detrimental conditions as well as a temporal heterogeneity of resources availability throughout the plant life cycle. We therefore hypothesized that a dynamic regulation of negative and positive systemic pathways regulating nodulation should exist to fine-tune nodule number depending on nutrient availability. We then analyzed the genetic interaction between CRA2 and SUNN pathways. To this aim, we first identified and characterized a *cra2* mutant allelic series in the *M. truncatula* Jemalong A17 genotype where a presumptive null *sunn* mutant allele was previously reported (*sunn-4*; Saur et al., 2011; Mortier et al., 2012). This allowed us to generate a *cra2 sunn* double mutant to analyze the genetic interaction between these two systemic pathways. We additionally tested interactions between AON-related CLE peptides and the CRA2 pathway. Finally, as the nitrate inhibition of nodule numbers is

lost in the *sunn* mutant, we analyzed how *cra2* and *cra2 sunn* mutant nodulation was affected by nitrate.

RESULTS

The *cra2* Mutant Forms an Increased Number of Lateral Roots and a Reduced Number of Symbiotic Nodules

Forward genetic screens in a *Tnt1* insertional mutant collection generated in the *M. truncatula* Jemalong A17-2HA genotype and in a γ -ray mutant collection generated in the Jemalong A17 genotype were performed to identify mutants showing a compact root system architecture phenotype (so-called *cra*; Fig. 1A). As mutants with a *cra* phenotype were previously identified in the *M. truncatula* R108 genotype and shown to be affected in an LRR-RLK referred to as MtCRA2 (Huault et al., 2014), the entire MtCRA2 locus was sequenced in the five *cra* mutant lines recovered. Genetic lesions were identified in the MtCRA2 coding region in these five allelic lines, corresponding to insertions of a transposon in the *cra2-11* and *cra2-14* alleles, to a nucleotide insertion in the *cra2-12* allele leading to a frame shift, or to nucleotide substitutions in the *cra2-13* (previously

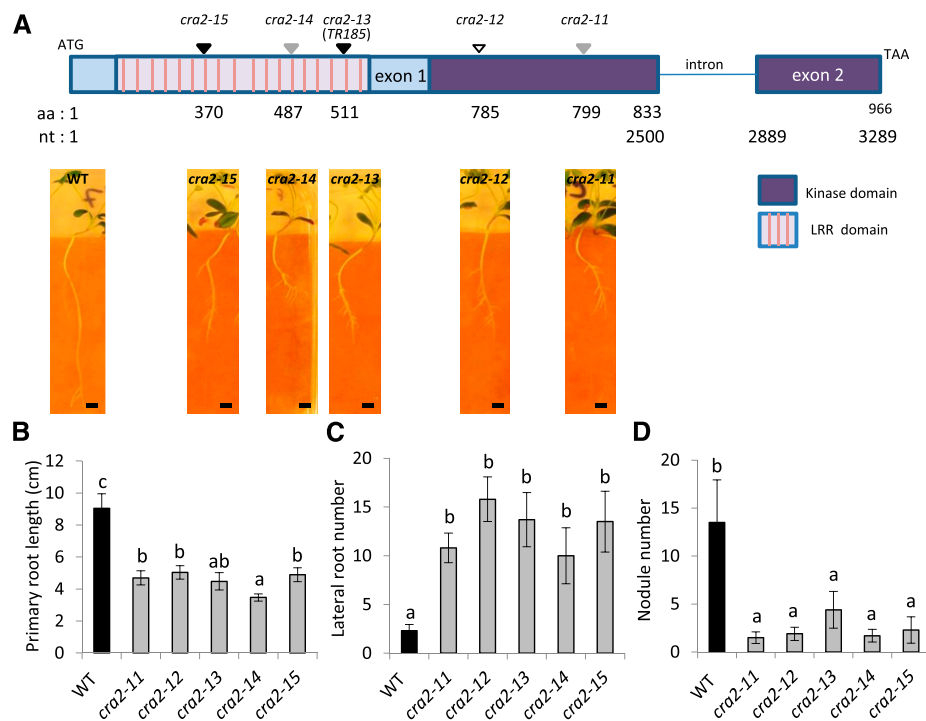


Figure 1. Identification of *cra2* mutant alleles in the *M. truncatula* Jemalong A17 genotype. A, Localization of transposon insertions (gray arrowheads), a nucleotide insertion (white arrowhead), or point mutations (black arrowheads) in *cra2* mutants identified in the *M. truncatula* Jemalong A17 genotype, as well as representative images of the phenotypes of the mutant alleles grown in vitro on a low-N medium for 14 d. aa, Amino acid; nt, nucleotide. Bars = 0.5 cm. B, Quantification of the primary root length of wild-type (WT) or *cra2-11* to *cra2-15* mutant plants grown in vitro on a low-N medium. C, Quantification of the lateral root number of wild-type or *cra2-11* to *cra2-15* mutant plants grown in vitro on a low-N medium. D, Quantification of nodule number of wild-type or *cra2-11* to *cra2-15* mutant plants 4 weeks postinoculation with rhizobium. In B to D, error bars represent confidence intervals ($\alpha = 0.05$; $n = 10$), and a Kruskal-Wallis test was used to assess significant differences, as indicated by lowercase letters ($\alpha < 0.01$). One representative biological experiment out of two is shown.

named *TR185*; Bourion et al., 2014) and *cra2-15* alleles (Supplemental Fig. S1A). These mutations consequently introduced premature stop codons in the LRR region (at positions 487 and 511 in *cra2-14* and *cra2-13* alleles, respectively), in the kinase domain (at positions 785 and 799 in *cra2-12* and *cra2-11* alleles, respectively), or in an Asn-to-Tyr amino acid conversion in the LRR region at position 370 in the case of the *cra2-15* allele (Fig. 1A; Supplemental Fig. S1B).

To evaluate the strength of these different *cra2* mutant alleles, a quantification of root length and of the number of lateral roots was performed, revealing that all mutants similarly have a shorter primary root (Fig. 1B) as well as an increased number of emerged lateral roots (Fig. 1C). Despite this strong root phenotype, *cra2* mutant plants grown on N-rich medium were not dwarfs, as illustrated 2 months after germination in Supplemental Figure S2A. In agreement with this, quantification of shoot dry weight at the end of the plant growth cycle was not significantly different from that of wild-type plants (Supplemental Fig. S2B).

The symbiotic nodulation phenotype of the different *cra2* alleles was then analyzed, revealing that all mutant alleles developed a similarly lower number of nodules (Fig. 1D), indicating that the five Jemalong A17 alleles are also similar for their nodule phenotypic strength. To determine if the *cra2* low-nodulation phenotype may be the consequence of a shoot growth defect, we quantified shoot and root biomass in a nodulation kinetic from 8 d postinoculation (dpi) with rhizobium to 35 dpi (Supplemental Fig. S3). This analysis revealed that at the early stage (8 dpi), a lower number of nodules was already detected in *cra2* mutants (Supplemental Fig. S3A), whereas their shoot and root biomass was not significantly different from the wild type (Supplemental Fig. S3, B–D). At later stages, shoot and root biomass of the *cra2* mutants becomes significantly lower.

We additionally analyzed the nodule weight of *cra2* mutant nodules, which was similar to the wild type (Supplemental Fig. S4A). We then assessed the capacity of the nodules to fix atmospheric N using an acetylene reduction assay (ARA; Supplemental Fig. S4, B and C). Even though, overall, *cra2* plants had a significantly reduced ability to fix atmospheric N due to the lower number of nodules formed (Supplemental Fig. S4D), *cra2* nodules maintained a wild-type capacity to fix N when the nodule weight was considered to normalize ARA (specific ARA activity; Supplemental Fig. S4B). This was in agreement with the observation that both wild-type and *cra2* mutant nodules have a similar elongated shape and a pink color associated with leghemoglobin pigments that are required for an active N fixation (Supplemental Fig. S4E).

Early Symbiotic Signaling, Rhizobial Infections, and Spontaneous Nodule Formation Are Reduced in *cra2* Mutants

To determine which early symbiotic processes were altered in the *cra2* mutant, we analyzed successively

their ability to (1) activate an early nodulation response, (2) become infected by rhizobia, and (3) form so-called spontaneous nodules independently of the presence of rhizobia. The expression of the *MtENOD11* symbiotic marker was first analyzed by real-time reverse transcription (RT)-PCR shortly after rhizobium inoculation, revealing that the induction observed in wild-type roots was reduced in *cra2* mutants (Fig. 2A). However, the comparison of expression levels between 1 and 2 dpi with rhizobium suggested rather a delayed response in the *cra2* mutant than an inability to perceive rhizobial bacteria and to activate an early symbiotic response.

We then analyzed if the number and progression of symbiotic ITs were affected in *cra2* mutants, using a rhizobium strain constitutively expressing a *LacZ* marker. An overall reduced number of ITs was detected in *cra2* roots, and the number of ITs that reached the root epidermis or the root cortex was lower than in wild-type roots (Fig. 2B). This suggests that the *cra2* mutant has a reduced ability to be infected by symbiotic rhizobia.

Finally, the ability of *cra2* mutants to form nodules in the absence of symbiotic bacteria was evaluated in roots ectopically expressing the kinase domain of the *Does Not Make Infections2/Symbiosis Receptor Kinase* (*DMI2/SYMRK*) early symbiotic gene, previously shown to efficiently induce the formation of spontaneous nodules in *M. truncatula* and other legumes, which are notably characterized by a peripheral vasculature similar to infected N-fixing nodules (Ried et al., 2014; Saha et al., 2014; Fig. 2C). *cra2* mutants formed significantly fewer spontaneous nodules in the absence of rhizobia than wild-type plants (Fig. 2D), indicating that independently of a symbiotic bacterial infection trigger, the ability to form nodules is reduced in *cra2* mutants.

CRA2 Regulates Antagonistically Lateral Root Formation and Symbiotic Nodule Formation and Is Required for MtCEP1 Peptide Action

To determine if the CRA2 pathway regulates nodule and lateral root number depending on its activity on roots and/or shoots, we performed grafting experiments with *cra2-11* and *cra2-12* alleles (Fig. 3; Supplemental Fig. S5). The compact root phenotype was observed only in grafting combinations associating *cra2* mutant roots with wild-type shoots (Fig. 3, A and B; Supplemental Fig. S5, A and B), indicating that CRA2 activity is required in roots to regulate root system architecture. No significant difference in shoot dry weight was observed between the various grafting combinations (Fig. 3, C and D; Supplemental Fig. S5, C and D), suggesting that the compact root architecture phenotype is not indirectly caused by a major shoot growth phenotype. Concerning nodulation, only the *cra2*/wild-type grafts showed the low-nodulation phenotype (Fig. 3, B and E; Supplemental Fig. S5, B and E), indicating that CRA2 activity is required in shoots to systemically regulate nodule

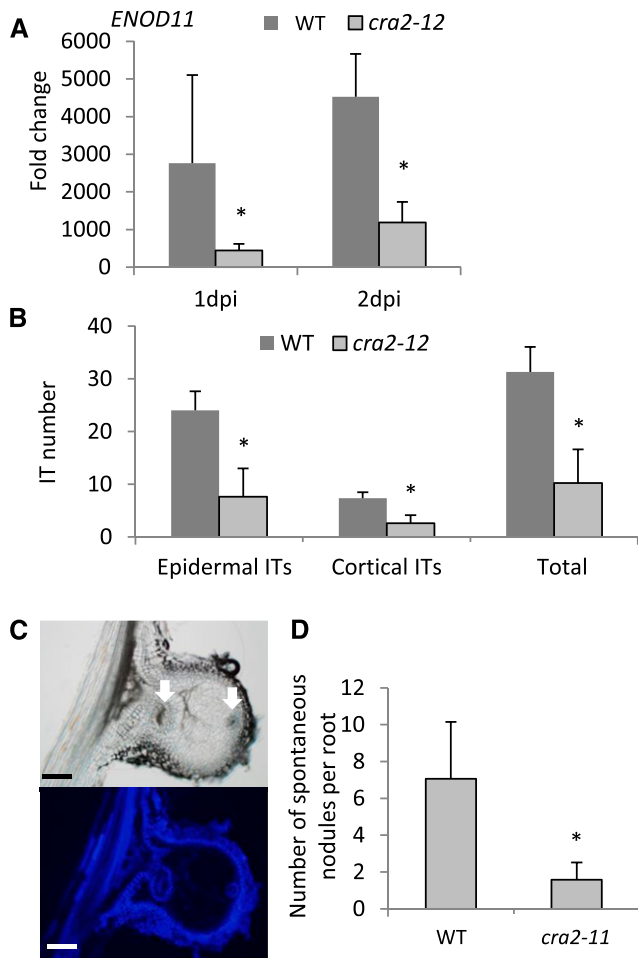


Figure 2. *ENOD11* expression, ITs, and spontaneous nodule number are reduced in *cra2* mutants. **A**, Expression analysis by real-time RT-PCR of the early nodulation marker *MtENOD11* in wild-type (WT) or *cra2-12* roots 1 or 2 dpi with rhizobium, normalized relative to expression levels in uninoculated control roots. Error bars represent *SD* from one representative biological experiment out of three. A Mann-Whitney test was used to assess significant differences indicated by asterisks ($\alpha < 0.05$; $n = 2$). **B**, Quantification of IT number in wild-type and *cra2-12* roots 6 dpi with a rhizobium strain constitutively expressing a LacZ reporter. ITs that reached the epidermis (Epidermal ITs) were distinguished from ITs that reached the cortex (Cortical ITs). Error bars represent confidence intervals ($\alpha = 0.05$; $n = 5$), and a Mann-Whitney test was used to assess significant differences, as indicated by asterisks ($\alpha < 0.05$). One representative biological experiment out of two is shown. **C**, Representative images of a section (50 μm) of a spontaneous nodule induced by the ectopic expression of a SYMRK-KD construct, in bright field (top) or under UV illumination (bottom) to visualize the blue autofluorescence of lignified cells and of the endodermis. White arrows indicate vascular bundles. Bars = 100 μm . **D**, Number of spontaneous nodules induced by the ectopic expression of a SYMRK-KD construct, per root of wild-type or *cra2-11* plants grown on a low-N medium for 5 weeks without rhizobium inoculation. Error bars represent confidence intervals ($\alpha = 0.05$; $n > 9$), and a Mann-Whitney test was used to assess significant differences, as indicated by the asterisk ($\alpha < 0.01$). One representative biological experiment out of two is shown.

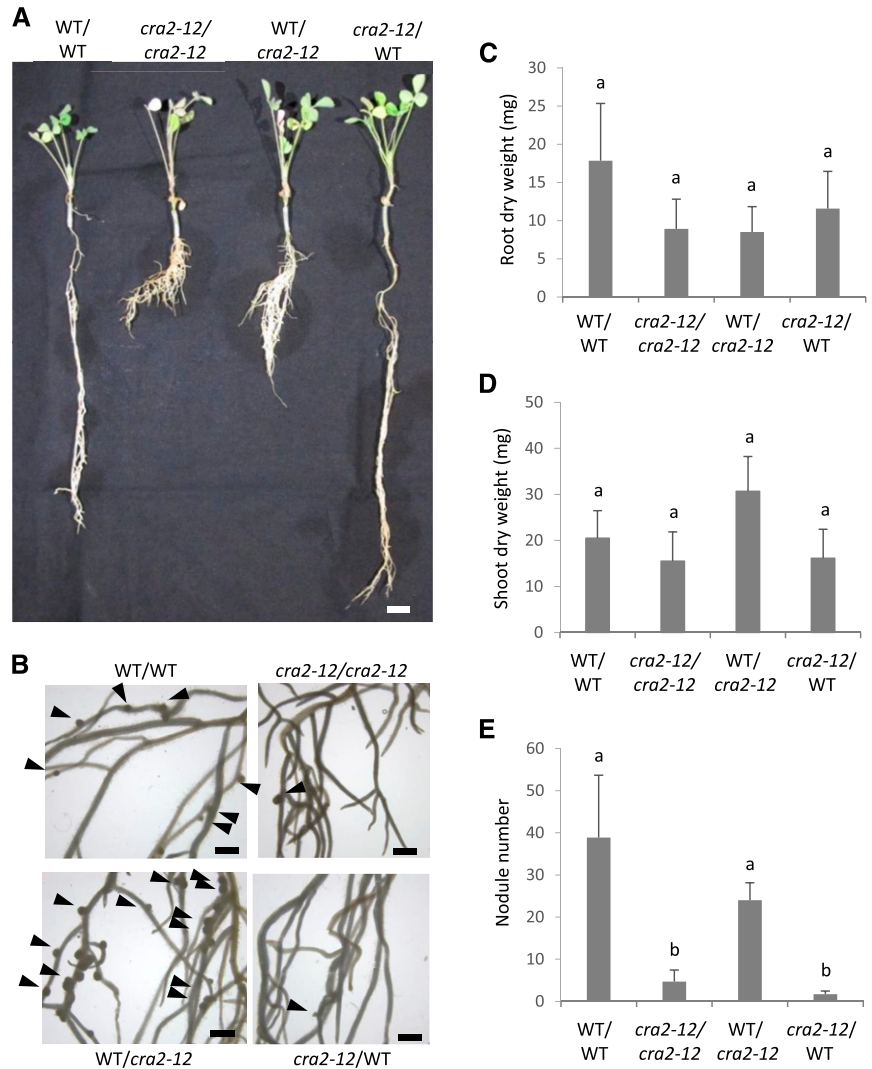
number. Finally, the link with MtCEP signaling peptides was tested. An exogenous treatment with MtCEP1 peptides significantly decreased lateral root number and conversely increased nodule number in the wild type, and these two responses were abolished in *cra2* mutants (Fig. 4).

SUNN and CRA2 Pathways Act Independently to Regulate Nodule Number

To determine if a genetic interaction exists between the systemic positive CRA2 and negative SUNN pathways regulating nodulation, we generated *cra2 sunn* double mutants by crossing the *cra2-11* mutant with the *sunn-4* presumptive null allele available in the Jemalong A17 genotype (Mortier et al., 2012). Nodulation phenotyping revealed that *cra2* and *sunn* single mutants develop fewer and more nodules, respectively, than wild-type plants, as expected (Fig. 5, A–C). The *cra2 sunn* double mutant formed an intermediate number of nodules between *cra2* and *sunn* single mutants, which was also significantly different from wild-type plants (~ 2.5 -fold higher). It was noticed that compared with wild-type plants, the nodule number in *cra2* mutants is decreased by a factor of about 3, whereas the nodule number is increased in *sunn* mutants by a factor of about 7. Thus, this likely explains that the nodule number in the *cra2 sunn* double mutant is approaching but not similar to the nodule number of wild-type plants. Interestingly, *cra2 sunn* double mutants develop a number of nodules that is even higher than wild-type plants despite a compact root architecture phenotype equivalent to that of *cra2* single mutants, as illustrated by representative images for each genotype in Figure 5B. This result first unambiguously demonstrates that the *cra2* mutation does not affect the ability of plants to form nodules but instead decreases their number, and second, that CRA2 and SUNN pathways independently regulate nodule number positively and negatively, respectively.

As an alternative to demonstrate relationships between CRA2 and SUNN systemic pathways, wild-type and *cra2* roots were transformed with an RNA interference (RNAi) construct designed to silence either GUS as a negative control or the *MtCLE13* gene previously shown to encode peptides negatively regulating nodule number depending on the SUNN receptor (Mortier et al., 2012). As expected, down-regulation of *MtCLE13* expression (Supplemental Fig. S6A) increased nodule number in wild-type plants (Fig. 5D). In the *cra2* mutant, an increased nodulation was similarly observed, indicating that the negative regulation of nodule number exerted by MtCLE13 peptides occurs independently or downstream of the CRA2 LRR-RLK receptor. Conversely, wild-type roots ectopically expressing *MtCLE13* (Supplemental Fig. S6B) strongly decreased the number of nodules in wild-type plants, as expected (Fig. 5E), compared with a non-nodulation-related

Figure 3. Symbiotic nodule number is controlled by CRA2 activity in shoots and lateral root number by CRA2 activity in roots. A, Representative images of different grafting combinations between wild-type (WT) or *cra2-12* plants grown in a perlite-sand mixture on a low-N medium 2 weeks postinoculation with rhizobium. Shoot/root grafting combinations are indicated above each plant. Bar = 2 cm. B, Details of nodulated roots of the different grafting combinations shown in A. Arrowheads indicate nodules. Bars = 0.2 cm. C, Quantification of the root dry weight (in milligrams) of the different wild-type/*cra2* grafting combinations. D, Quantification of the shoot dry weight (in milligrams) of the different wild-type/*cra2* grafting combinations. E, Quantification of the nodule number of the different wild-type/*cra2* grafting combinations. In C to E, error bars represent confidence intervals ($\alpha = 0.05$; $n > 9$), and a Kruskal-Wallis test was used to assess significant differences, as indicated by lower-case letters ($\alpha < 0.05$). One representative biological experiment out of two is shown.



MtCLE4 gene used as a negative control (Mortier et al., 2010). These results indicate that the inhibitory action of MtCLE13 peptides on nodulation is not compromised in *cra2* mutants.

The Nitrate Inhibition of Nodulation Occurs in *cra2* Mutants But Not in *sunm* or *cra2 sunm* Mutants

As the *sunm* mutant was previously reported to form more nodules than wild-type plants, not only in low-N conditions but also in the presence of N (Sagan et al., 1995), we tested if the nodulation capacity of the *cra2* and *cra2 sunm* mutants was affected or not by a nitrate treatment. The number of nodules was then comparatively analyzed in plants grown on a medium supplemented with 0.1 mM (low N) or 10 mM (high N) KNO_3 (Fig. 6A). On low N, the nodulation phenotype of all mutants grown in vitro was similar to the one previously observed with plants grown in a pot (Fig. 5, A–C), as illustrated in Figure 6B. On high N, the nodule number was reduced in wild-type plants, as expected,

as well as in *cra2* mutants, despite its already low-nodulation phenotype (Fig. 6A). In contrast, the nodule number in *sunm* mutants was not affected by nitrate, as previously reported (Sagan et al., 1995), and the *cra2 sunm* double mutant behaved similarly to the *sunm* mutant. These results indicate that the negative regulation of nodulation exerted by nitrate is still acting in *cra2* mutants and that this regulation is lost in *sunm* and *cra2 sunm* mutants.

DISCUSSION

In this study, we identified *M. truncatula* mutants affecting the CRA2 LRR-RLK receptor involved in the systemic regulation of legume root system architecture. This revealed an early defect in the regulation of nodulation affecting the interaction from the primary steps (i.e. symbiotic signaling and rhizobial infections). These new mutants also allowed to analyze relationships of the CRA2 systemic pathway with the SUNN systemic pathway negatively regulating symbiotic nodulation.

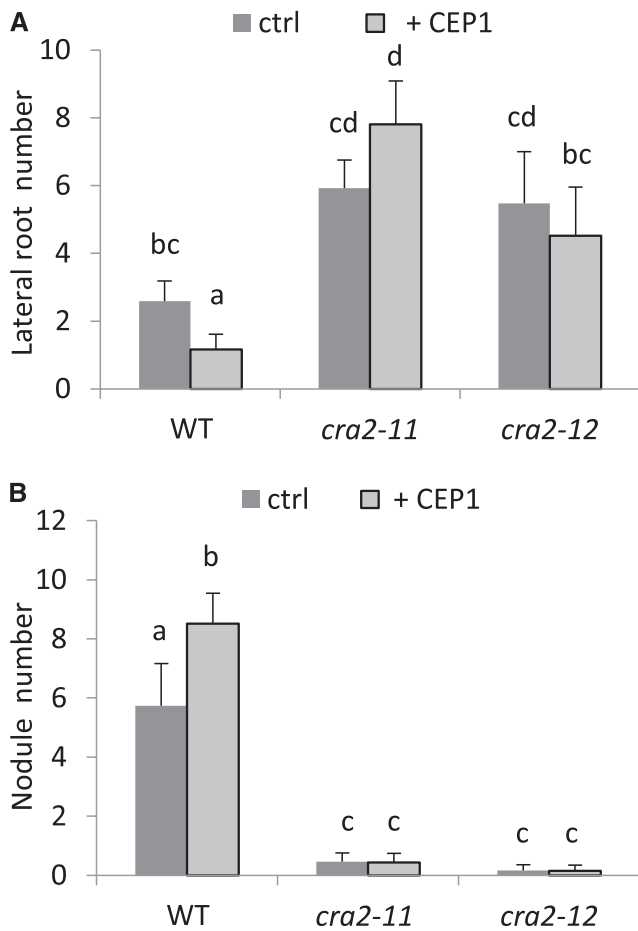


Figure 4. MtCEP1 peptides decrease lateral root number and increase nodule number depending on the CRA2 receptor. A, Quantification of the lateral root number of wild-type (WT), *cra2-11*, or *cra2-12* plants grown in vitro on a low-N medium for 14 d with or without MtCEP1 peptides. Error bars represent confidence intervals ($\alpha = 0.05$; $n > 20$), and a Kruskal-Wallis test was used to assess significant differences, as indicated by lowercase letters ($\alpha < 0.05$). B, Quantification of the nodule number of wild-type, *cra2-11*, or *cra2-12* plants grown in vitro on a low-N medium for 14 dpi with rhizobium with or without MtCEP1 peptides. Error bars represent confidence intervals ($\alpha = 0.05$; $n > 20$), and a Kruskal-Wallis test was used to assess significant differences, as indicated by lowercase letters ($\alpha < 0.05$). One representative biological experiment out of three is shown.

Finally, as the *summ* mutant has an excessive nodulation also under nitrate inhibitory conditions, we tested the relationship between nitrate and these systemic pathways.

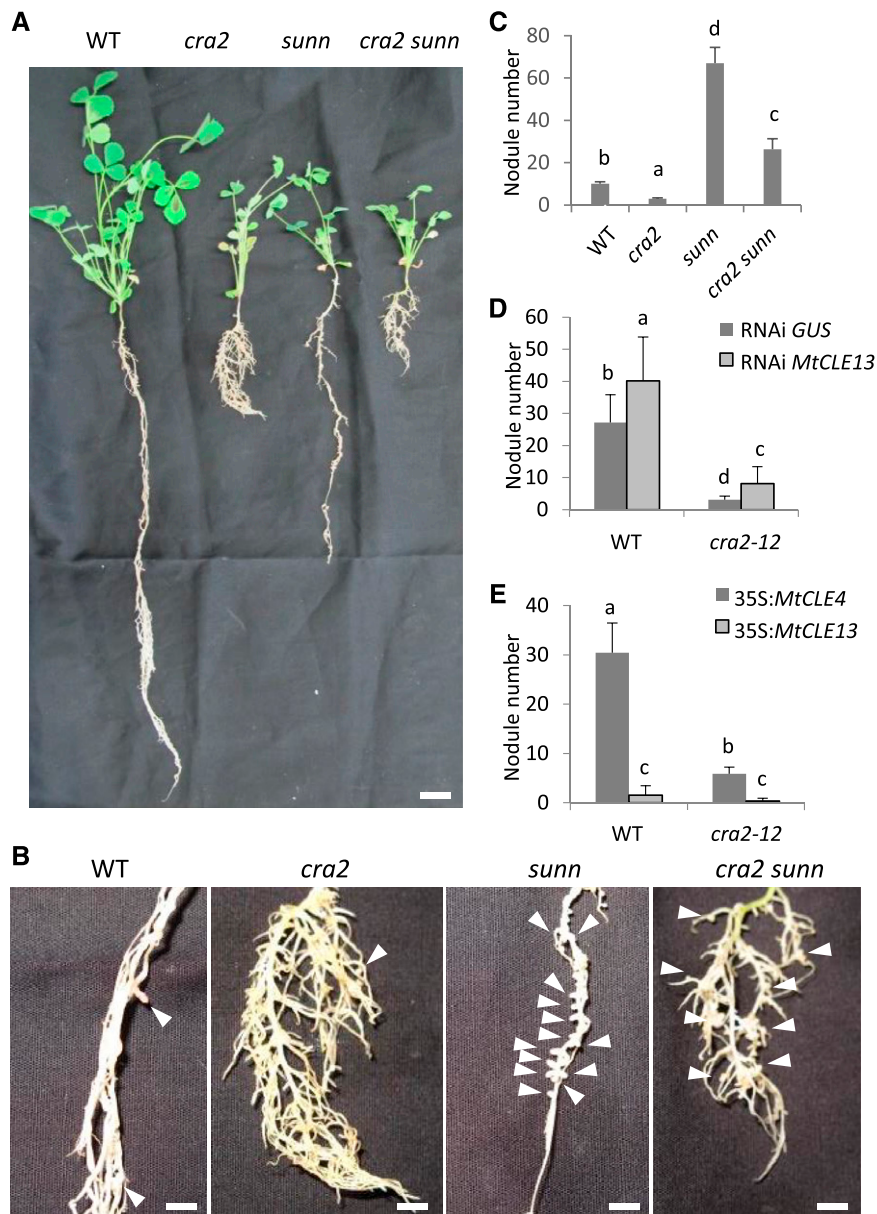
To characterize the new *cra2* allelic series identified, we evaluated the strength of root and nodulation phenotypes. All five Jemalong A17 *cra2* mutant alleles have a similarly reduced root growth, increased lateral root branching, and reduced nodule number, in agreement with phenotypes previously reported in the *M. truncatula* R108 genotype (Huault et al., 2014). The strength of the five alleles is therefore independent of the location and of the nature of mutations (transposon insertion or nucleotide

substitution/insertion leading to frame shifts in most of the cases), suggesting that they are null alleles. Interestingly, the nucleotide substitution in the *cra2-15* allele led to an Asn-to-Tyr amino acid conversion at position 370, which suggests a functional role of this specific residue.

Discrepancies between grafting results were reported for *cra2* mutants identified in different genotypes, R108 (Huault et al., 2014) or Jemalong A17 for the *cra2-13* allele previously referred to as *TR185* (Bourion et al., 2014). Indeed, the compact root architecture phenotype was either linked to CRA2 activity in roots in R108 alleles (Huault et al., 2014) or to shoot control in Jemalong A17 (Bourion et al., 2014), whereas in both genotypes, the *cra2* low-nodulation phenotype was linked to CRA2 activity in shoots (Huault et al., 2014; this study). In this study, we now show using different *cra2* mutant alleles in the Jemalong A17 genotype, *cra2-11*, and *cra2-12*, but also *cra2-13/TR185*, that the compact root phenotype is root controlled, as previously observed in the R108 genotype. This result was validated by PCR genotyping of the CRA2 locus in the different grafted plant combinations to unambiguously separate successful grafts from adventitious root contaminations that are prone to form in the Jemalong A17 genotype, in contrast to the R108 genotype. The formation of adventitious roots with a high frequency in the grafting junction of Jemalong A17 plants likely explains the discrepancy with the Bourion et al. (2014) study, wherein the verification of the genotype of the grafts was not possible as the causal mutation was not known. In agreement with the phenotype of lateral root number controlled locally by roots, the effect of MtCEP1 peptides on lateral root formation was observed in Jemalong A17 isolated hairy roots missing shoots (Mohd-Radzman et al., 2015). Finally, the antagonistic effect of MtCEP1 peptides on lateral root and nodule numbers requires the CRA2 receptor acting in roots and shoots, respectively, both in Jemalong A17 and R108 *M. truncatula* genotypes (Huault et al., 2014; Mohd-Radzman et al., 2016; this study). This result is consistent with the identification in Arabidopsis of AtCEPR1 and AtCEPR2 receptors, most closely related to MtCRA2, as required for the systemic regulation of AtCEP1 target genes (Huault et al., 2014; Tabata et al., 2014).

It remained unclear from previous studies conducted in the R108 genotype (Huault et al., 2014) which root symbiotic processes were affected by the CRA2 systemic pathway. To more precisely evaluate the nodulation phenotype of *cra2* mutants, we analyzed the three main stages of nodule initiation classically defined: the symbiont recognition (preinfection) stage; the rhizobium infection stage initially affecting epidermal root hairs and then the root cortex; and nodule organogenesis occurring in the inner cortex in *M. truncatula*. To determine which of these processes was affected in *cra2* mutants, we analyzed (1) the expression of one of the most specific early-nodulation markers, *ENOD11*; (2) the number and progression of ITs; and (3) the number of spontaneous nodule organs that can form in the

Figure 5. SUNN and CRA2 pathways act independently to regulate nodule number. **A**, Representative images of wild-type (WT), *cra2*, *sunn*, or *cra2 sunn* mutant plants grown in a perlite-sand mixture on low-N medium 4 weeks postinoculation with rhizobium. Bar = 2 cm. **B**, Detail of nodulated roots of the different mutants shown in **A**. Arrowheads indicate nodules. Bars = 0.5 cm. **C**, Quantification of nodule number of wild-type, *cra2*, *sunn*, or *cra2 sunn* mutant plants grown as described in **A**. Error bars represent confidence intervals ($\alpha = 0.05$; $n > 20$), and a Kruskal-Wallis test was used to assess significant differences, as indicated by lowercase letters ($\alpha < 0.01$). One representative biological experiment out of three is shown. **D**, Quantification of the nodule number of wild-type or *cra2-12* plants expressing an RNAi construct driven by the 35S Cauliflower mosaic virus promoter and targeting either *GUS* as a negative control or the *MtCLE13* gene. Plants were grown in a perlite-sand mixture on low-N medium, and nodules were quantified 4 weeks postinoculation with rhizobium. Error bars represent confidence intervals ($\alpha = 0.05$; $n > 15$), and a Kruskal-Wallis test was used to assess significant differences, as indicated by lowercase letters ($\alpha < 0.05$). One representative biological experiment out of two is shown. **E**, Quantification of the nodule number of wild-type or *cra2-12* plants overexpressing (35S Cauliflower mosaic virus) either the *MtCLE13* gene or the nonnodulation-related *MtCLE4* gene as a negative control. Plants were grown in a perlite-sand mixture on low-N medium, and nodules were quantified 4 weeks postinoculation with rhizobium. Error bars represent confidence intervals ($\alpha = 0.05$; $n > 10$), and a Kruskal-Wallis test was used to assess significant differences, as indicated by lowercase letters ($\alpha < 0.05$). One representative biological experiment out of two is shown.



absence of a rhizobial trigger. These three parameters were affected in *cra2* mutants, suggesting that multiple symbiotic stages may be targeted by the CRA2 systemic pathway. In agreement with an action on rhizobial infections, MtCEP1 peptides, previously shown to act depending on the CRA2 receptor, conversely increased the number of symbiotic ITs formed as well as N fixation and nodulation at moderate levels of nitrate (Imin et al., 2013; Mohd-Radzman et al., 2016). When analyzing later nodulation phenotypes, such as nodule size and capacity to reduce atmospheric N, a similar phenotype to wild-type nodules was identified in *cra2* mutant nodules, as observed for alleles in the R108 genotype (Huault et al., 2014). This therefore confirms that a primary function of the CRA2 pathway is to regulate the number of nodules but not their differentiation or metabolic activity.

A major reason to generate this novel *cra2* allelic series in the Jemalong A17 genotype was to analyze genetic interactions between the SUNN and CRA2 antagonistic systemic pathways regulating nodulation using the *sunn-4* mutant, a presumptive null allele available only in this genotype (Saur et al., 2011; Mortier et al., 2012). Analysis of the nodulation phenotype of *cra2 sunn* double mutants revealed a nodule number intermediate between the two single mutants. Interestingly, this unambiguously shows that the CRA2 pathway regulates the number of nodules but is not required per se to form a nodule, as *cra2* mutants can still generate a wild-type number of nodules in the *sunn* mutant background. This result is consistent with grafting outcomes, as the wild type/*cra2* grafting combination formed a wild-type number of nodules on a highly branched root system, highlighting that *cra2*

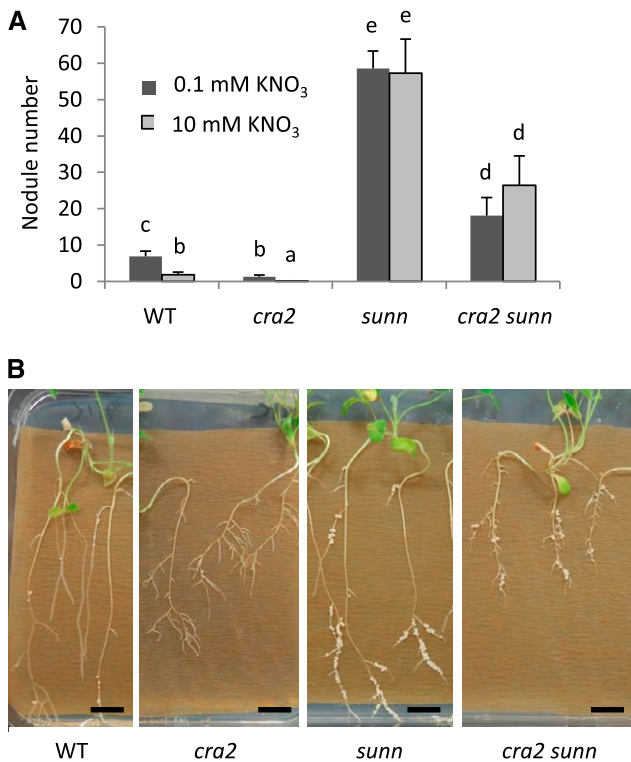


Figure 6. Nodulation phenotypes of *cra2 sunn* double mutants in low or high N. A, Quantification of the nodule number of wild-type (WT), *cra2*, *sunn*, or *cra2 sunn* mutant plants grown in vitro with 0.1 or 10 mM KNO₃ 14 dpi with rhizobium. Error bars represent confidence intervals ($\alpha = 0.05$; $n > 15$), and a Kruskal-Wallis test was used to assess significant differences indicated by lowercase letters ($\alpha < 0.05$). One representative biological experiment out of two is shown. B, Representative images of nodulated wild-type, *cra2*, *sunn*, or *cra2 sunn* mutant plants. Bars = 1 cm.

mutant roots can recover a wild-type ability to nodulate when grafted onto wild-type shoots. The *cra2 sunn* nodulation phenotype additionally strongly suggests that the CRA2 and SUNN pathways act independently. This is in agreement with previous results showing that MtCEP1 peptides can still increase nodulation in the *sunn* supernodulation mutant (Mohd-Radzman et al., 2016). Conversely, we now show that the strong inhibition of nodulation exerted by the MtCLE13 ectopic expression is still occurring in the already low-nodulating *cra2* mutant, indicating that this AON-related CLE peptide acts independently of the CRA2 pathway. Strikingly, both CRA2 and CLE13/SUNN pathways antagonistically affect the NF induction of the *ENOD11* marker in *M. truncatula* (Mortier et al., 2010; this study). However, an independent action of CRA2 and SUNN signaling to antagonistically regulate nodule number does not exclude that a coordination between these systemic pathways exists over time, notably depending on soil N availability and on the plant C/N metabolic status, as suggested both in *M. truncatula* and *Arabidopsis* (Imin et al., 2013; Araya et al., 2014a, 2014b; Tabata et al., 2014). Further work is thus needed to determine at which level such coordination between these systemic regulations might exist.

Finally, in contrast to *cra2* mutant alleles in the R108 genotype that were nearly nonnodulating, *cra2* Jemalong A17 alleles still form some nodules, even though to a much lower extent than wild-type plants. This allowed testing the relevance of the CRA2 pathway in relation to the inhibitory effect of nitrate on nodulation. Indeed, previous studies reported that a nitrate treatment strongly inhibiting nodulation in wild-type plants was not able to inhibit *sunn* excessive nodulation, suggesting that the *sunn* nodulation is nitrate tolerant (Schnabel et al., 2005; Jeudy et al., 2010). *cra2* nodulation was still inhibited by nitrate, whereas nodulation of *sunn* and of the *cra2 sunn* double mutant was nitrate tolerant. This suggests that the nitrate control of nodule number seems at best partially overlapping with the systemic regulation of nodule number. In agreement with this result, depending on plant species, a nitrate-local or systemic negative regulation of nodulation was reported in soybean and in *L. japonicus*, respectively (Reid et al., 2011; Okamoto and Kawaguchi, 2015). In *M. truncatula*, depending on the N source used, local and systemic regulations of nodule number and function have been reported, and the SUNN pathway was

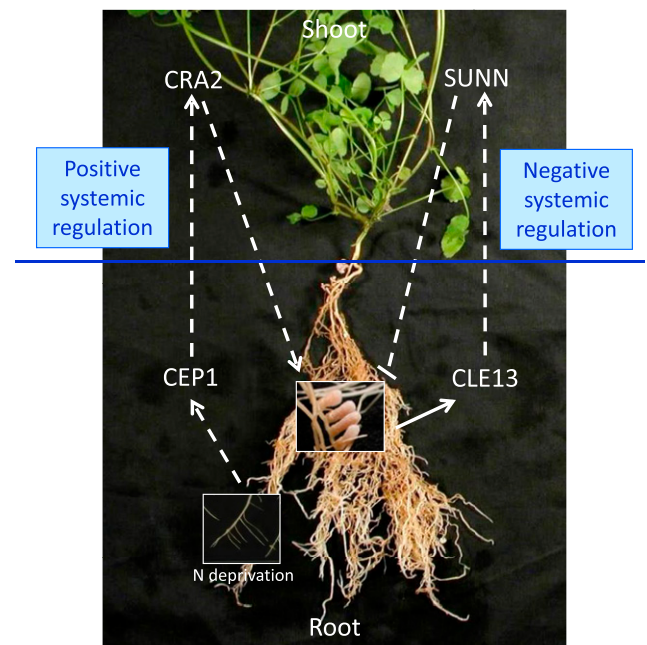


Figure 7. A model for the systemic regulation of symbiotic nodulation in *M. truncatula*. The positive systemic regulation of nodulation is initiated in N-deficient roots by the production of CEP peptides that would be transported to shoots through the xylem to activate the CRA2 CEPR-like receptor, leading to the production of a downstream systemic signal positively regulating nodulation in roots. In the presence of compatible rhizobia, symbiotic nodulation is triggered and leads to the production of specific CLE peptides such as MtCLE13 that would be transported to shoots through the xylem to act depending on the SUNN CLAVATA1-like receptor, leading to the production of a downstream systemic signal negatively regulating nodulation in roots. These two pathways act independently of each other to systemically regulate nodulation depending on N and rhizobium availability.

linked to the systemic inhibition of nodule number by nitrate (Jeudy et al., 2010).

CONCLUSION

The antagonistic CEP/CRA2 and CLE/SUNN pathways systemically regulating nodulation from shoots act independently, pointing to a working model where under N-limiting conditions, the production of several CEP peptides (Imin et al., 2013), acting through the CRA2 receptor in shoots, generates a downstream signal(s) positively affecting the nodulation capacity of roots by regulating notably NF signaling and rhizobial infections (Fig. 7). In response to compatible rhizobia, nodule primordia initiate and AON-related CLE peptides are produced, leading to the SUNN-dependent activation in shoots of inhibitory shoot-to-root systemic signals (Fig. 7). Further work is needed to determine more precisely which potential signaling peptides are involved, beyond the already characterized MtCEP1 and MtCLE12/MtCLE13 peptides, and how their production is dynamically coordinated over time depending on soil N availability and whole-plant metabolic capacity and needs. Finally, systemic molecular signals and targets of SUNN and CRA2 pathways linked to nodule initiation should be identified to determine if some of those can be common and which nodulation stages are targeted.

MATERIALS AND METHODS

Biological Material and Growth Conditions

The *cra2* mutants were identified by a forward genetics approach carried out in community screens of the *Tnt1* insertional mutant collection generated in the *Medicago truncatula* Jemalong A17 (2HA) genotype for *cra2-11* and *cra2-14* alleles (Domonkos et al., 2017) or in a γ -ray mutant collection generated in the Jemalong A17 genotype for the *cra2-12*, *cra2-13/TR185* (Bourion et al., 2014), and *cra2-15* alleles. The *sunm-4* mutant allele was isolated by Sagan et al. (1995). The *cra2 sunm* double mutant was generated in this study by crossing *cra2-11* and *sunm-4* alleles. The PCR genotyping of homozygous *cra2* and *cra2 sunm* mutants was achieved using primers indicated in Supplemental Table S1. PCR amplification products were sequenced for the different mutant alleles.

In all cases, *M. truncatula* seeds were scarified in sulfuric acid (Sigma) for 3 min, washed four times with distilled water, and then sterilized for 20 min in bleach (12% [v/v] sodium hypochlorite). After washing with sterilized water, seeds were sown onto 1.5% (w/v) water-agar plates (Bactoagar; Becton Dickinson), stratified for 2 d in the dark at 4°C, and then germinated overnight at 24°C. Germinated seedlings were grown in vitro vertically in a growth chamber at 24°C under a long-day photoperiod (16 h of light, 150 μ E intensity) on square plates on a Fahraeus low-N medium (Truchet et al., 1989). Low-N versus high-N experiments were performed in vitro on a Fahraeus medium supplemented with 0.1 or 10 mM KNO₃, respectively. Alternatively, germinated seedlings were grown in pots containing a perlite:sand 3:1 mixture watered every 2 d with i medium (Blondon, 1964) in a growth chamber (24°C, 16 h of light, 150 μ E, relative humidity of 60%). Finally, to perform a full growth cycle and quantify biomass, plants were grown on soil watered with SN/2 N-rich medium in a greenhouse (Gonzalez-Rizzo et al., 2006).

For nodulation experiments, the *Sinorhizobium meliloti* 1021 strain (Sm1021) was used for in vitro experiments or the *Sinorhizobium medicae* WSM419 strain for plants grown in perlite/sand pots and notably for ARA experiments, as this strain was previously shown to be a better N fixer than Sm1021 (Terpolilli et al., 2008). Sm1021 (GMI6526; Ardourel et al., 1994) carrying a pXLGD4 plasmid expressing a *Pro_{HemA}:LacZ* marker was used to follow bacterial progression

from root hairs to cortical cells and quantify infection phenotypes. A β -galactosidase histochemical assay was performed overnight on 5-dpi roots as described by Ardourel et al. (1994). Stained roots were observed using a stereomicroscope (Olympus, BX53). *Sinorhizobium* strains were grown at 28°C on a yeast extract broth medium (Vervliet et al., 1975) supplemented with 50 mg L⁻¹ streptomycin, 25 mg L⁻¹ chloramphenicol, or 10 mg L⁻¹ tetracycline for Sm1021, WSM419, and Sm1021-*LacZ* strains, respectively. Plants were inoculated with an OD_{600nm} = 0.05 dilution.

Constructs and *Agrobacterium rhizogenes*-Mediated Root Transformation

An RNAi construct targeting the *MtCLE13* gene was generated by introducing a 200-nucleotide *MtCLE13* PCR product into the pEntr/D-Topo vector (Life Technologies) and then recombined (Gateway technology) into the pFRN vector (Gonzalez-Rizzo et al., 2006) and checked by sequencing (primers indicated in Supplemental Table S1). The GUS RNAi pFRN control vector was previously described by Gonzalez-Rizzo et al. (2006). The 35S:CLE13 and 35S:CLE4 vectors were previously generated by Mortier et al. (2010). The SYMRK-KD vector allowing an efficient formation of spontaneous nodules in *M. truncatula* was previously described by Saha et al. (2014).

Constructs of interest were introduced into the *A. rhizogenes* Arqua1 strain, and recombinant Arqua1 bacteria were used to transform roots according to the protocol described by Boisson-Dernier et al. (2001). The *A. rhizogenes* strains were grown at 28°C for 2 d on a yeast extract broth-agar medium supplemented with streptomycin and kanamycin (50 mg L⁻¹). Infected seedlings were grown in vitro on a Fahraeus medium supplemented with 1 mM NH₄NO₃ (Truchet et al., 1989) and with kanamycin (25 mg L⁻¹) for 1 week at 20°C, and another 1 week at 24°C, under a 16-h-light photoperiod (150 μ E intensity). Then, composite plants with wild-type shoots and transformed roots selected on kanamycin were transferred either in vitro on growth paper (Mega International) dropped off on Fahraeus without N agar medium, grown for 5 d, and then inoculated with the Sm1021 strain as described before, or transferred in pots containing a perlite:sand 3:1 mixture for 5 d and then inoculated with the WSM419 strain as described before. For generating spontaneous nodules, 35S:SYMRK-KD composite plants were transferred in vitro on a Fahraeus low-N medium without rhizobium inoculation, and spontaneous nodules were scored 5 weeks after transfer. Sections (50 μ m) of spontaneous nodule were obtained using a vibratome (Leica, VTS1200) on 3% agarose (Sigma)-embedded material and imaged with a stereomicroscope (Olympus, BX53) in a bright field or under UV illumination.

Root and Nodule Phenotyping

Nodule number was either scored on seedlings grown in vitro at 14 dpi with rhizobium or in pots at time points indicated in the figure legends. Lateral root number was scored on seedlings grown in vitro at 14 d postgermination. Primary root length was measured using ImageJ software (<http://imagej.nih.gov>).

Peptide exogenous treatments were performed by adding 1 μ M MtCEP1 to the low-N Fahraeus medium or to Fahraeus medium supplemented with 5 mM KNO₃ for nodulation or lateral root phenotyping experiments, respectively, according to Imin et al. (2013).

Grafting

Grafts were generated as described in the *Medicago Handbook* (chapter Cuttings and Grafts; <http://www.noble.org/medicagohandbook/>). Grafts were generated in vitro and then transferred after 3 weeks to pots containing a perlite:sand 3:1 mixture and watered with a low-N liquid medium, in the same growth conditions as previously described. Grafts were inoculated 1 week after the transfer, and the nodule number was scored 2 weeks postinoculation with rhizobium. Root and shoot dry weights were measured after drying in an oven at 60°C for 48 h. As in the Jemalong A17 genotype, grafted junctions were highly prone to form adventitious roots, roots were genotyped to determine their CRA2 wild-type versus homozygous mutant status, allowing exclusion of adventitious root contaminations. Details of nodulated roots were imaged using an AxioZoom V16 microscope (Zeiss).

Real-Time RT-PCR Gene Expression Analysis

Total RNA was isolated from frozen roots with the RNeasy Plant mini kit (Qiagen) according to the manufacturer's instructions. Total RNAs (1.5 μ g) were

used for cDNA synthesis with SuperScript II Reverse Transcriptase (Thermo Fisher). RT-quantitative PCR experiments were performed with a LightCycler480 SYBR Green I Master Kit on a LightCycler 480 apparatus (Roche Diagnostics) according to the manufacturer's instructions. Cycling conditions were 95°C for 10 min followed by 40 cycles at 95°C for 15 s, 60°C for 15 s, and 72°C for 15 s. A threshold for minimal efficiency was set at 90% to retain primers. A dissociation curve (55°C–95°C) was performed to assess the specificity of the amplification, and amplicons were additionally sequenced. The expression of the genes of interest was normalized against the reference genes *MtACTIN11* and *MtRBP1* (*RNA BINDING PROTEIN1*) previously selected using the Genorm software (<https://genorm.cmgg.be/>; Vandensompele et al., 2002). All primers used in real-time RT-PCR are indicated in Supplemental Table S1. Values obtained for the two reference genes were averaged to calculate ratios, and the value of the experimental control condition was set to 1 as a reference to determine fold changes.

N Fixation Activity

The nitrogenase activity of symbiotic nodules was evaluated through an ARA performed on individual plants, as reported by Koch and Evans (1966). Briefly, plants grown in pots with a perlite:sand 3:1 mixture were harvested 4 weeks after inoculation with rhizobium and placed into glass vials sealed with rubber septa. Acetylene was injected into each vial and incubated for 3 h at 22°C before injection into the gas chromatographer (7820A; Agilent Technologies) to determine the amount of ethylene produced by the nodule nitrogenase activity. The total ARA activity was calculated as nanomoles of ethylene produced per hour per plant. The specific ARA activity was determined by normalizing ARA values with the nodule fresh weight (in milligrams). A negative control was performed by incubating acetylene with noninoculated plants.

Statistical Analyses

Two to three independent biological replicates were performed. Nonparametric tests (available in the Xlstat software; <http://www.xlstat.com/>) were used to assess significant differences: a Mann-Whitney test when two conditions were compared, and a Kruskal-Wallis test when more than two conditions were considered.

Accession Numbers

Sequence data from this article can be found in the GenBank/EMBL data libraries under accession numbers Medtr3g110840 (*M. truncatula* genome version 4.0, <https://phytozome.jgi.doe.gov/pz/portal.html>; Tang et al., 2014) or MtrunA17Chr3g0140861 (*M. truncatula* genome version 5.0, <https://medicago.toulouse.inra.fr/MtrunA17r5.0-ANR/>; Pecrix et al., 2018) for MtCRA2; Medtr4g070970 or MtrunA17Chr4g0035451 for MtSUNN; Medtr4g079610 or MtrunA17Chr4g0040951 for MtCLE13; Medtr3g415670 or MtrunA17Chr3g0082991 for MtENOD11; Medtr6g034835 or MtrunA17Chr6g0463441 for MtRBP1; and Medtr7g026230 or MtrunA17Chr7g0223901 for MtACTIN11.

Supplemental Data

The following supplemental materials are available.

Supplemental Figure S1. Localization of mutations in the different *cra2* Jemalong A17 mutant alleles.

Supplemental Figure S2. Shoot growth phenotypes of *cra2* mutants.

Supplemental Figure S3. The *cra2* low-nodulation phenotype is detected before scoring for shoot or root biomass phenotypes.

Supplemental Figure S4. N fixation capacity of *cra2* mutant nodules and plants.

Supplemental Figure S5. Symbiotic nodule number is controlled by CRA2 activity in shoots and lateral root number by CRA2 activity in roots.

Supplemental Figure S6. *MtCLE13* expression in RNAi or overexpressing roots.

Supplemental Table S1. Primers used in this study.

ACKNOWLEDGMENTS

We thank Krisztina Miró, Sandor Jenei, Ágota Domonkos, Aniko Gombár, Beatrix Horváth, Gyongyi Kovács, and Szilard Kovács for participating in screening *Tnt1* insertional mutant alleles in the frame of the French-Hungarian bilateral NKTH-ANR LEGUMICS project. Insertional mutants were generated in the frame of the EU Grain Legumes Integrated Project. We thank Henri de Larambergue and Véronique Aubert for participating in screening the γ -ray mutant collection at the Agroécologie Institute (Institut National de la Recherche Agronomique). We thank Maitrayee DasGupta (Kolkata, India) and Sofie Goormachtig (Ghent, Belgium) for providing 35S:SYMRK-KD and 35S:CLE4/35S:CLE13 plasmids, respectively. Microscopy was done at the Institute of Plant Sciences Paris-Saclay imaging facility.

Received January 3, 2019; accepted February 6, 2019; published February 19, 2019.

LITERATURE CITED

- Araya T, Miyamoto M, Wibowo J, Suzuki A, Kojima S, Tsuchiya YN, Sawa S, Fukuda H, von Wirén N, Takahashi H (2014a) CLE-CLAV-ATA1 peptide-receptor signaling module regulates the expansion of plant root systems in a nitrogen-dependent manner. *Proc Natl Acad Sci USA* **111**: 2029–2034
- Araya T, von Wirén N, Takahashi H (2014b) CLE peptides regulate lateral root development in response to nitrogen nutritional status of plants. *Plant Signal Behav* **9**: e29302
- Ardourel M, Demont N, Debellé F, Maillat F, de Billy F, Promé JC, Dénarié J, Truchet G (1994) *Rhizobium meliloti* lipooligosaccharide nodulation factors: Different structural requirements for bacterial entry into target root hair cells and induction of plant symbiotic developmental responses. *Plant Cell* **6**: 1357–1374
- Blondin F (1964) Contribution à l'Étude du Développement des Graminées Fourragères Ray-grass et Dactyle. Faculté des Sciences, Paris
- Boisson-Dernier A, Chabaud M, Garcia F, Bécard G, Rosenberg C, Barker DG (2001) *Agrobacterium rhizogenes*-transformed roots of *Medicago truncatula* for the study of nitrogen-fixing and endomycorrhizal symbiotic associations. *Mol Plant Microbe Interact* **14**: 695–700
- Bourion V, Martin C, de Larambergue H, Jacquin F, Aubert G, Martin-Magniette ML, Balzergue S, Lescure G, Citerne S, Lepetit M, et al (2014) Unexpectedly low nitrogen acquisition and absence of root architecture adaptation to nitrate supply in a *Medicago truncatula* highly branched root mutant. *J Exp Bot* **65**: 2365–2380
- Caetano-Anollés G, Gresshoff PM (1991) Plant genetic control of nodulation. *Annu Rev Microbiol* **45**: 345–382
- Carroll BJ, McNeil DL, Gresshoff PM (1985) A supernodulation and nitrate-tolerant symbiotic (nts) soybean mutant. *Plant Physiol* **78**: 34–40
- de Bang TC, Lundquist PK, Dai X, Boschiero C, Zhuang Z, Pant P, Torres-Jerez I, Roy S, Nogales J, Veerappan V, et al (2017) Genome-wide identification of *Medicago* peptides involved in macronutrient responses and nodulation. *Plant Physiol* **175**: 1669–1689
- De Kroon H, Visser EJW, Huber H, Mommer L, Hutchings MJ (2009) A modular concept of plant foraging behaviour: The interplay between local responses and systemic control. *Plant Cell Environ* **32**: 704–712
- Domonkos Á, Kovács S, Gombár A, Kiss E, Horváth B, Kovács GZ, Farkas A, Tóth MT, Ayaydin F, Bóka K, et al (2017) NAD1 controls defense-like responses in *Medicago truncatula* symbiotic nitrogen fixing nodules following rhizobial colonization in a BacA-independent manner. *Genes (Basel)* **8**: E387
- Giehl RFH, von Wirén N (2014) Root nutrient foraging. *Plant Physiol* **166**: 509–517
- Gonzalez-Rizzo S, Crespi M, Frugier F (2006) The *Medicago truncatula* CRE1 cytokinin receptor regulates lateral root development and early symbiotic interaction with *Sinorhizobium meliloti*. *Plant Cell* **18**: 2680–2693
- Hastwell AH, Richard J, Corcilius L, Williams JT, Gresshoff PM, Ferguson BJ (2019) Triarabinsylation is required for nodulation-suppressive CLE peptides to systemically inhibit nodulation in *Pisum sativum*. *Plant Cell Environ* **42**: 188–197
- Huault E, Laffont C, Wen J, Mysore KS, Ratet P, Duc G, Frugier F (2014) Local and systemic regulation of plant root system architecture and symbiotic nodulation by a receptor-like kinase. *PLoS Genet* **10**: e1004891

- Imin N, Mohd-Radzman NA, Ogilvie HA, Djordjevic MA (2013) The peptide-encoding CEP1 gene modulates lateral root and nodule numbers in *Medicago truncatula*. *J Exp Bot* **64**: 5395–5409
- Imin N, Patel N, Corcilius L, Payne RJ, Djordjevic MA (2018) CLE peptide tri-arabinylation and peptide domain sequence composition are essential for SUNN-dependent autoregulation of nodulation in *Medicago truncatula*. *New Phytol* **218**: 73–80
- Jardinaud MF, Boivin S, Rodde N, Catrice O, Kisiala A, Lepage A, Moreau S, Roux B, Cottret L, Sallet E, et al (2016) A laser dissection-RNAseq analysis highlights the activation of cytokinin pathways by Nod factors in the *Medicago truncatula* root epidermis. *Plant Physiol* **171**: 2256–2276
- Jeuzy C, Ruffel S, Freixes S, Tillard P, Santoni AL, Morel S, Journet EP, Duc G, Gojon A, Lepetit M, et al (2010) Adaptation of *Medicago truncatula* to nitrogen limitation is modulated via local and systemic nodule developmental responses. *New Phytol* **185**: 817–828
- Journet EP, El-Gachtouli N, Vernoud V, de Billy F, Pichon M, Dedieu A, Arnould C, Morandi D, Barker DG, Gianinazzi-Pearson V (2001) *Medicago truncatula* ENOD11: A novel RPRP-encoding early nodulin gene expressed during mycorrhization in arbuscule-containing cells. *Mol Plant Microbe Interact* **14**: 737–748
- Koch B, Evans HJ (1966) Reduction of acetylene to ethylene by soybean root nodules. *Plant Physiol* **41**: 1748–1750
- Krusell L, Madsen LH, Sato S, Aubert G, Genua A, Szczyglowski K, Duc G, Kaneko T, Tabata S, de Bruijn F, et al (2002) Shoot control of root development and nodulation is mediated by a receptor-like kinase. *Nature* **420**: 422–426
- Malamy JE (2005) Intrinsic and environmental response pathways that regulate root system architecture. *Plant Cell Environ* **28**: 67–77
- Mohd-Radzman NA, Binos S, Truong TT, Imin N, Mariani M, Djordjevic MA (2015) Novel MtCEP1 peptides produced in vivo differentially regulate root development in *Medicago truncatula*. *J Exp Bot* **66**: 5289–5300
- Mohd-Radzman NA, Laffont C, Ivanovici A, Patel N, Reid D, Stougaard J, Frugier F, Imin N, Djordjevic MA (2016) Different pathways act downstream of the CEP peptide receptor CRA2 to regulate lateral root and nodule development. *Plant Physiol* **171**: 2536–2548
- Mortier V, Den Herder G, Whitford R, Van de Velde W, Rombauts S, D'Haeseleer K, Holsters M, Goormachtig S (2010) CLE peptides control *Medicago truncatula* nodulation locally and systemically. *Plant Physiol* **153**: 222–237
- Mortier V, De Wever E, Vuylsteke M, Holsters M, Goormachtig S (2012) Nodule numbers are governed by interaction between CLE peptides and cytokinin signaling. *Plant J* **70**: 367–376
- Nishida H, Handa Y, Tanaka S, Suzuki T, Kawaguchi M (2016) Expression of the CLE-RS3 gene suppresses root nodulation in *Lotus japonicus*. *J Plant Res* **129**: 909–919
- Oh E, Seo PJ, Kim J (2018) Signaling peptides and receptors coordinating plant root development. *Trends Plant Sci* **23**: 337–351
- Okamoto S, Kawaguchi M (2015) Shoot HAR1 mediates nitrate inhibition of nodulation in *Lotus japonicus*. *Plant Signal Behav* **10**: e1000138
- Okamoto S, Ohnishi E, Sato S, Takahashi H, Nakazono M, Tabata S, Kawaguchi M (2009) Nod factor/nitrate-induced CLE genes that drive HAR1-mediated systemic regulation of nodulation. *Plant Cell Physiol* **50**: 67–77
- Okamoto S, Shinohara H, Mori T, Matsubayashi Y, Kawaguchi M (2013) Root-derived CLE glycopeptides control nodulation by direct binding to HAR1 receptor kinase. *Nat Commun* **4**: 2191
- Oldroyd GED (2013) Speak, friend, and enter: Signalling systems that promote beneficial symbiotic associations in plants. *Nat Rev Microbiol* **11**: 252–263
- Pecrix Y, Staton SE, Sallet E, Lelandais-Brière C, Moreau S, Carrère S, Blein T, Jardinaud MF, Latrasse D, Zouine M, et al (2018) Whole-genome landscape of *Medicago truncatula* symbiotic genes. *Nat Plants* **4**: 1017–1025
- Reid DE, Ferguson BJ, Gresshoff PM (2011) Inoculation- and nitrate-induced CLE peptides of soybean control NARK-dependent nodule formation. *Mol Plant Microbe Interact* **24**: 606–618
- Ried MK, Antolin-Llovera M, Parniske M (2014) Spontaneous symbiotic reprogramming of plant roots triggered by receptor-like kinases. *eLife* **3**: 01600
- Sagan M, Morandib D, Tarenghib E, Due G (1995) Selection of nodulation and mycorrhizal mutants in the model plant *Medicago truncatula* (Gaertn.) after γ -ray mutagenesis. *Plant Sci* **111**: 63–71
- Saha S, Dutta A, Bhattacharya A, DasGupta M (2014) Intracellular catalytic domain of symbiosis receptor kinase hyperactivates spontaneous nodulation in absence of rhizobia. *Plant Physiol* **166**: 1699–1708
- Saur IM, Oakes M, Djordjevic MA, Imin N (2011) Crosstalk between the nodulation signaling pathway and the autoregulation of nodulation in *Medicago truncatula*. *New Phytol* **190**: 865–874
- Schnabel E, Journet EP, de Carvalho-Niebel F, Duc G, Frugoli J (2005) The *Medicago truncatula* SUNN gene encodes a CLV1-like leucine-rich repeat receptor kinase that regulates nodule number and root length. *Plant Mol Biol* **58**: 809–822
- Searle IR, Men AE, Laniya TS, Buzas DM, Iturbe-Ormaetxe I, Carroll BJ, Gresshoff PM (2003) Long-distance signaling in nodulation directed by a CLAVATA1-like receptor kinase. *Science* **299**: 109–112
- Suzuki T, Yoro E, Kawaguchi M (2015) Leguminous plants: Inventors of root nodules to accommodate symbiotic bacteria. *Int Rev Cell Mol Biol* **316**: 111–158
- Tabata R, Sumida K, Yoshii T, Ohyama K, Shinohara H, Matsubayashi Y (2014) Perception of root-derived peptides by shoot LRR-RKs mediates systemic N-demand signaling. *Science* **346**: 343–346
- Tang H, Krishnakumar V, Bidwell S, Rosen B, Chan A, Zhou S, Gentzbittel L, Childs KL, Yandell M, Gundlach H, et al (2014) An improved genome release (version Mt4.0) for the model legume *Medicago truncatula*. *BMC Genomics* **15**: 312
- Tavormina P, De Coninck B, Nikonorova N, De Smet I, Cammue BPA (2015) The plant peptidome: An expanding repertoire of structural features and biological functions. *Plant Cell* **27**: 2095–2118
- Terpolilli JJ, O'Hara GW, Tiwari RP, Dilworth MJ, Howieson JG (2008) The model legume *Medicago truncatula* A17 is poorly matched for N₂ fixation with the sequenced microsymbiont *Sinorhizobium meliloti* 1021. *New Phytol* **179**: 62–66
- Timmers ACJ, Auriac MC, Truchet G (1999) Refined analysis of early symbiotic steps of the *Rhizobium-Medicago* interaction in relationship with microtubular cytoskeleton rearrangements. *Development* **126**: 3617–3628
- Truchet G, Barker D, Camut S, de Billy F, Vasse J, Huguet T (1989) Alfalfa nodulation in the absence of *Rhizobium*. *Mol Gen Genet* **219**: 65–68
- Vandesompele J, De Preter K, Pattyn F, Poppe B, Van Roy N, De Paepe A, Speleman F (2002) Accurate normalization of real-time quantitative RT-PCR data by geometric averaging of multiple internal control genes. *Genome Biol* **3**: RESEARCH0034
- Vervliet G, Holsters M, Teuchy H, Van Montagu M, Schell J (1975) Characterization of different plaque-forming and defective temperate phages in *Agrobacterium*. *J Gen Virol* **26**: 33–48
- Xiao TT, Schilderink S, Moling S, Deinum EE, Kondorosi E, Franssen H, Kulikova O, Niebel A, Bisseling T (2014) Fate map of *Medicago truncatula* root nodules. *Development* **141**: 3517–3528